Lithos 386–387 (2021) 105999

Contents lists available at ScienceDirect

Lithos

journal homepage: www.elsevier.com/locate/lithos

Research Article

The Ordovician Thores volcanic island arc of the Pearya Terrane from northern Ellesmere Island formed on Precambrian continental crust

Jarosław Majka [a,b,*], Karolina Kośmińska [b], Jakub Bazarnik [c], William C. McClelland [d]

[a] Department of Earth Sciences, Uppsala University, Villavägen 16, SE-752 36 Uppsala, Sweden
[b] Faculty of Geology, Geophysics and Environmental Protection, AGH – University of Science and Technology, al. Mickiewicza 30, 30-059 Kraków, Poland
[c] Polish Geological Institute – National Research Institute, Carpathian Branch, ul. Skrzatów 1, 31-560 Kraków, Poland
[d] Department of Earth and Environmental Sciences, University of Iowa, Iowa City, IA 52242, USA

ARTICLE INFO

Article history:
Received 10 August 2020
Received in revised form 12 January 2021
Accepted 14 January 2021
Available online 23 January 2021

Keywords:
Zircon
Caledonides
High Arctic
Iapetus

ABSTRACT

Ion microprobe U–Pb zircon dating of intermediate to felsic rocks coupled with bulk-rock geochemistry analyses and compared to previously published data shows that the Thores Suite of the Pearya Terrane of northern Ellesmere Island (Arctic Canada) represents an Early Ordovician (c. 490–470 Ma) suite formed in an island arc setting. Interestingly, three out of five dated samples contain abundant xenocrystic zircon that have ages spanning from c. 2690 Ma to c. 520 Ma. The vast majority of xenocrystic zircon are Precambrian in age and typical of Laurentia. The youngest well-pronounced age cluster around 580–570 Ma is inferred to be an expression of the Timanide Orogen, traditionally ascribed to Baltica. This geochronological dataset provides new insight on the origin of the Thores Suite of the Pearya Terrane, which was traditionally thought to be formed due to the M'Clintock orogenic event and commonly treated as independent from Caledonian tectonism. We suggest that the Thores island arc formed on a sliver of continental crust within the Iapetus Ocean. The timing of igneous activity recorded by the Thores Suite is consistent with other island arcs and subduction-related metamorphic units that occur within the Caledonides of northern Scandinavia and Svalbard. Hence, we suggest that the Thores volcanic island arc was closely associated with age equivalent arcs developed within the northern Iapetus Ocean. Its juxtaposition with the other successions of the Pearya Terrane is explained by a large-scale, left lateral, strike-slip system operating along the northeastern margins of Baltica and Laurentia, coeval with the main collision between the two continents. This strike-slip system was responsible for the juxtaposition of multiple terranes with contrasting Precambrian histories that can be traced in the present day High Arctic, e.g. in southwest Svalbard and the Pearya Terrane.

1. Introduction

The early stages of Iapetus Ocean closure involved formation of intraoceanic island arcs subsequently followed by subduction of continental crustal lithologies of the adjacent continents. In the North Atlantic region, evidence for this process is especially well preserved within the Middle and Upper allochthons of the Scandinavian Caledonides that bear multiple occurrences of late Cambrian/early Ordovician high pressure (HP) and island arc rocks (e.g. Gee et al., 2013). These HP units are the relicts of the subducted Iapetus oceanic and Baltica continental plates, whereas the island arc lithologies represent intra-Iapetus suprasubduction zone magmatism. High pressure rocks of broadly similar age are also known from the Svalbard Caledonides in the high Arctic (e.g. Barnes et al., 2020; Bernard-Griffiths et al., 1993; Hirajima et al., 1988; Peucat et al., 1989), but the upper plate of the subduction system in which they formed (island arc or active continental margin) is not preserved in-situ. The only early Paleozoic volcanic arc complex thus far recognized in the high Arctic has been described in the composite Pearya Terrane of northern Ellesmere Island (Trettin et al., 1982) which formed due to collision of Meso- to Neoproterozoic crystalline and sedimentary lithologies of the Pearya Terrane Successions I and II with and island arc during the M'Clintock Orogeny (Trettin, 1991). Similarly, broadly coeval HP units from Svalbard may have formed by initial intra-Iapetus oceanic subduction and subsequent arc collision with a continental fragment of probable Laurentian affinity, thus providing a possible link between HP metamorphism in Svalbard and island arc magmatism preserved in the Pearya Terrane (e.g. Gee and Teben'kov, 2005; Labrousse et al., 2008; Majka et al., 2015).

We present U–Pb isotopic results of ion microprobe analysis of zircon from various felsic to intermediate lithologies in the Thores Suite within Succession III of the Pearya Terrane. These rocks have been interpreted as island arc lithologies juxtaposed with peri-Laurentian

* Corresponding author at: Department of Earth Sciences, Uppsala University, Villavägen 16, SE-752 36 Uppsala, Sweden.
E-mail address: jaroslaw.majka@geo.uu.se (J. Majka).

https://doi.org/10.1016/j.lithos.2021.105999
0024-4937/

basement during the M'Clintock Orogeny and dated to c. 488–480 Ma (Estrada et al., 2018a; Trettin et al., 1982). Our age estimates suggest arc magmatism extended over a longer time span through c. 469 Ma, overlapping with the proposed timing of the M'Clintock Orogeny. More importantly, some of the dated samples revealed the common occurrence of inherited cores within zircon that yielded older ages ranging from Neoarchean to Cambrian. Based on this discovery we suggest that the Thores Suite records arc-related magmatism located either at the northern Laurentia margin or on a sliver of Precambrian continental crust (i.e. microcontinent) within the Iapetus Ocean. The new data sheds new light on a character of the Thores Suite magmatism and allows us to formulate an alternative tectonic scenario that accommodates High Arctic subduction complexes within the 'Caledonian' realm without the need to involve a separate M'Clintock orogenic event.

2. Geological setting

The Pearya Terrane of northern Ellesmere Island (Fig. 1) is considered to be exotic to the Canadian and Greenland shields mostly because of the abundance of Tonian orthogneiss (e.g. Estrada et al., 2018a; Malone et al., 2017; Trettin, 1998). Pearya forms a composite terrane subdivided into five megaunits (Fig. 1) as follows: (a) Succession I dominated by Tonian orthogneiss and minor metasedimentary rocks, (b) Succession II comprising late Proterozoic to earliest Paleozoic (meta)sedimentary units and arc-related volcanics (Hadlari et al., 2014; Malone et al., 2014), (c) Succession III consisting of an arc complex including Early Ordovician ultramafic, mafic, intermediate and felsic rocks (Estrada et al., 2018a; Trettin, 1998) as well as associated (meta)sedimentary units; (d) Succession IV forming a sequence of Ordovician unmetamorphosed terrigenous and volcanoclastic sedimentary rocks, carbonate and calc-alkaline volcanic rocks (Trettin, 1998), and (e) Succession V comprised of late Ordovician to late Silurian marine sedimentary rocks that unconformably overlie Succession IV (Trettin, 1998). Succession III is divided into an unnamed metavolcanosedimentary sequence and the magmatic Thores Suite which is the focus of this study. The contact between the two Succession III units is poorly defined, but is most likely tectonic. Succession III is in fault contact with Successions II and IV.

The metavolcanosedimentary series consists of various metasedimentary lithologies differing in metamorphic grade, which may imply further tectonic subdivision of the unit. These rocks are represented by lower greenschists facies metatuffs and carbonate-chlorite-bearing tuffaceous slates as well as chloritoid-garnet-bearing schists. The latter are considerably higher in metamorphic grade, but it is unclear whether they are just amphibolite facies or represent an HP member of the Succession III. The slates occur with metabasalts of *E*-MORB affinity (Estrada et al., 2018a). U–Pb zircon dating of the lower greenschists facies metatuffs yielded a weighted average of c. 570 Ma for three samples and has been interpreted as an expression of possible intraoceanic Timanian arc volcanism (Estrada et al., 2018a). Other detrital zircon components in the samples span between c. 707 and 492 Ma, the latter defining a possible maximum depositional age for the metavolcanic units.

The Thores Suite consists of ultramafic rocks represented mainly by pyroxenites and peridotites, as well as gabbros, monzogabbros, monzodiorites, monzonites, quartz monzonites, trondhjemites and granodiorites (Estrada et al., 2018a; Trettin, 1998; Trettin et al., 1982). The two largest outcrops of these rocks are located west and east of M'Clintock Inlet, and referred to as the M'Clintock Body West and East, respectively (Figs. 1, 2; Table 1). Geochemically, the Thores Suite bears typical characteristics of subduction-related rocks and its mafic members follow trends of volcanic arc basalts (Estrada et al., 2018a). Limited Nd and Sr isotopic data from the Thores Suite rocks substantially differ from those derived for the *E*-MORB metabasalts of the metavolcanosedimentary unit (see Estrada et al., 2018a for more details). Conventional U–Pb zircon dating of a quartz monzonite yielded 481 + 7/−6 Ma (Trettin et al., 1982), whereas LA-ICP-MS zircon dating of two samples of monzonite yielded ages of 488 ± 2 Ma (Estrada et al., 2018a).

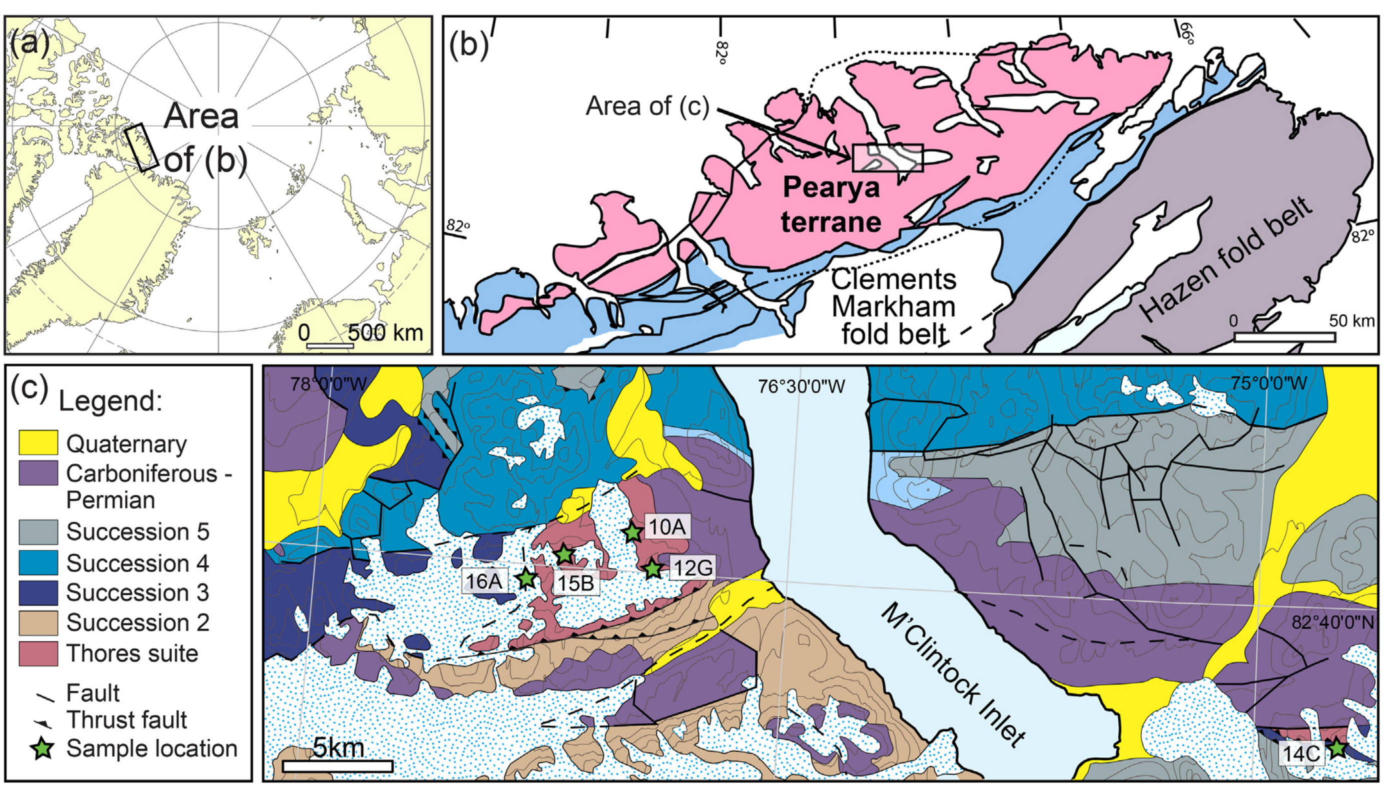

Fig. 1. (a) Circum-Arctic region with the location of the study area marked by a rectangle, (b) simplified geological map of northern Ellesmere Island (modified after Trettin, 1998), (c) Geological map of the M'Clintock Inlet area with the sample locations marked (modified after Trettin & Mayhr, 1996). GPS coordinates are listed in Table 1.

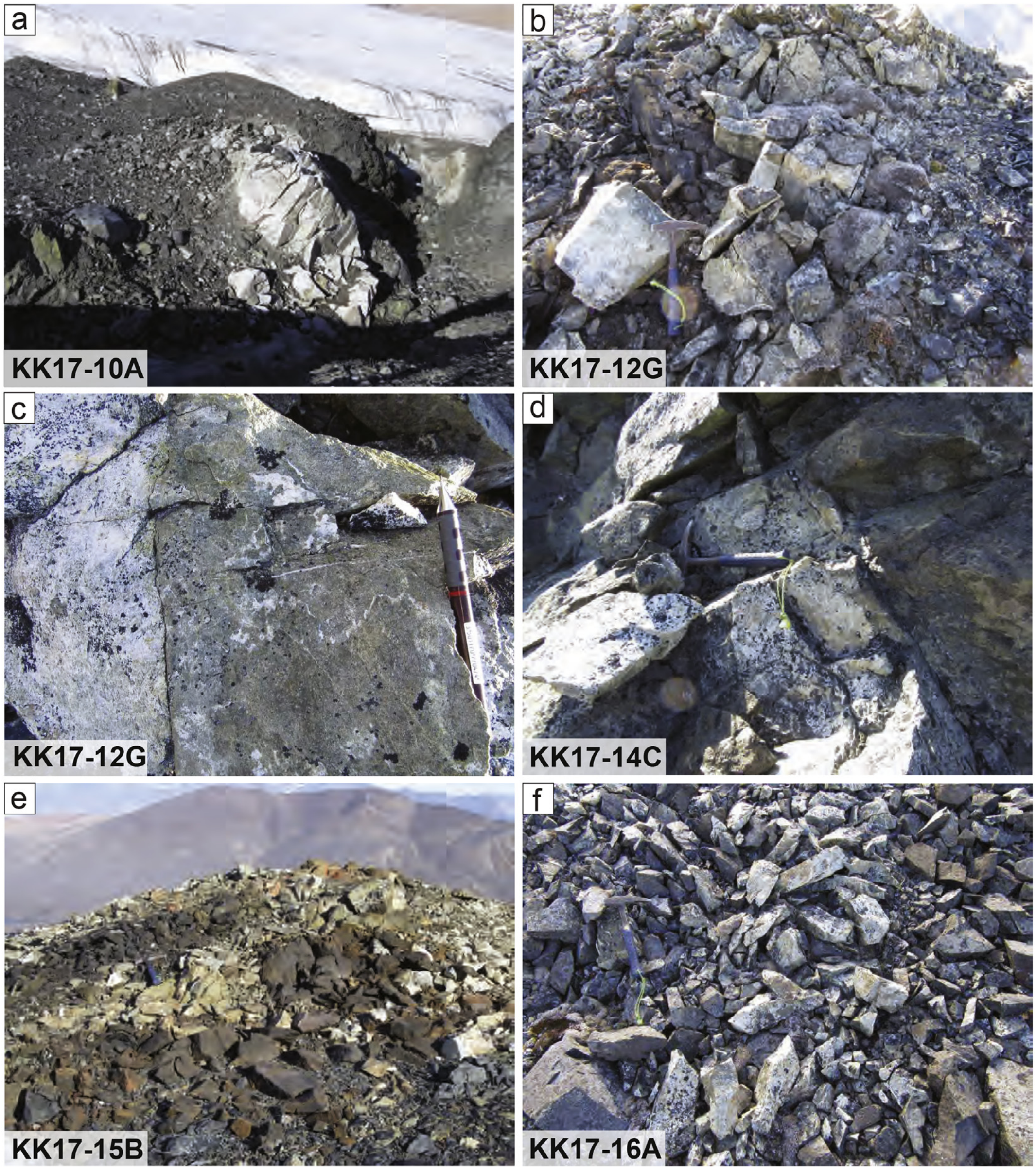

Fig. 2. Field photographs of the sampled rocks of the Thores Suite.

Table 1
Samples locations.

Sample ID	Lithology	GPS coordinates	Location
KK17 - 10A	Granite	82°41′03.1"N 76°59′56.1" W	M'Clintock West
KK17 - 12G	Q Monzonite	82°40′06.9"N 76°55′19.2" W	M'Clintock West
KK17 - 14C	Syenite	82°36′38.7"N 74°42′31.5" W	M'Clintock East
KK17 - 15B	Monzodiorite	82°40′21.1"N 77°12′44.9" W	M'Clintock West
KK17 - 16A	Granite	82°39′42.4"N 77°21′24.9" W	M'Clintock West

Estrada et al. (2018b) suggest that Succession III formed due to activation of Early Ordovician subduction beneath an ancient Timanian island arc covered by Cambrian sediments. This process led to formation of a new island arc that eventually collided with Successions I and II to form the composite Pearya Terrane during the M'Clintock orogeny. The location of the collision is inferred to be proximal to Laurentia based on similarities in detrital zircon signature of Succession II and the Franklinian margin (Malone et al., 2014). Docking of the island arc with Succession II was estimated to occur by c. 475 Ma (Trettin, 1998) based on the age of a syntectonic intrusion. This agrees with a single Ar–Ar hornblende step-heating age date derived by Estrada et al. (2018b) for one of the *E*-MORB basalts. The M'Clintock orogeny was supposed to be completed by c. 465 Ma based on the age of a post-tectonic intrusion (Trettin, 1991).

3. Methods

3.1. Whole-rock analyses

Major and trace element analyses were obtained for all samples selected for U–Pb zircon dating (see below) by inductively coupled plasma emission spectrometry (ICP-ES) and inductively coupled plasma mass spectrometry (ICP-MS) at the Bureau Veritas Mineral Laboratories, Canada according to their standard procedure (https://www.bvlabs.com/markets-services/mining/exploration-geochemistry). The geochemistry results are shown in Table 2.

3.2. Zircon analyses

U–Pb zircon geochronology using a sensitive high-resolution ion microprobe (SHRIMP IIe/MC) was performed at the Micro-Area Analysis Laboratory at the Polish Geological Institute – National Research Institute in Warszawa (Poland). Heavy mineral separates were obtained by standard crushing, grinding, magnetic and heavy liquid methods. Zircons for analysis were hand picked, comounted with standard reference materials Temora II (Black et al., 2004, 2003) and 91500 (Wiedenbeck et al., 1995; Wiedenbeck et al., 2004) in 2.5 cm epoxy mounts and polished to expose the grain interiors. The grains were imaged in cathodoluminescence (CL) using a HITACHI SU3500 scanning electron microscope.

U–Pb zircon dating followed the analytical procedures of Williams and Claesson (1987), Williams (1998) and Nawrocki et al. (2018.) The 91,500 zircon standard was used for calibration of U concentration and the Temora II standard was used to correct for U/Pb fractionation. Analyses were conducted with a 3.5 nA negative O2⁻ primary ion beam focused to ca. 23 μm diameter spot and a mass resolution ca. 6500.

Data reduction and plotting were performed using the SQUID Excel Macro of (Ludwig, 2000) and ISOPLOT (Ludwig, 2003). Age interpretations are based either on the measured $^{207}Pb/^{206}Pb$ ratio corrected for common Pb using the ^{204}Pb-method (see Williams, 1998) for zircon older than 1000 Ma or the measured $^{206}Pb/^{238}U$ ratio corrected for common Pb using the ^{207}Pb method for ages younger than 1000 Ma. The long-term reproducibility of Temora standard was 416.79 +- −0.54 Ma while the reproducibility during the analyses was 416.88 + −0.78 Ma.

Table 2
Major and trace element whole-rock results.

Sample ID	KK17 - 10A	KK17 - 12G	KK17 - 14C	KK17 - 15B	KK17 - 16A
Lithology	Granite	Q Monzonite	Syenite	Monzodiorite	Granite
SiO_2	69.72	67.22	58.41	54.32	70.12
TiO_2	0.17	0.12	0.14	0.15	0.14
Al_2O_3	15.98	17.60	20.69	21.61	15.87
FeO (tot)	1.60	1.62	2.39	3.82	1.86
MnO	0.03	0.03	0.06	0.05	0.07
MgO	0.27	0.58	0.30	1.69	0.50
CaO	1.56	1.14	3.74	9.78	2.57
Na_2O	7.74	7.94	6.72	5.17	6.93
K_2O	1.51	2.30	3.61	1.43	0.85
P_2O_5	0.04	0.07	0.05	0.08	0.05
LOI	1.30	1.30	2.60	2.00	0.80
Total	99.92	99.92	98.71	100.10	99.76
Rb	18.4	30.6	51.2	36.2	10.8
Sr	468.4	452.3	6371.1	1301.7	1009.3
Y	8.3	8.8	19.9	4.7	19.9
Zr	104.7	111.0	164.0	34.7	106.1
Nb	3.2	3.5	30.7	0.8	7.5
Cs	0.3	0.8	1.4	0.6	0.2
Ba	1232	922	6268	430	1997
La	15.5	14.8	145.6	12.6	25.4
Ce	26.7	23.7	258.3	17.2	45.9
Pr	2.81	2.19	26.20	1.65	4.93
Nd	9.7	7.7	84.2	6.1	17.7
Sm	1.43	1.38	11.46	1.09	3.14
Eu	0.49	0.37	2.96	0.47	0.76
Gd	1.41	1.29	7.81	1.00	3.15
Tb	0.22	0.20	0.91	0.14	0.50
Dy	1.35	1.31	4.09	0.91	3.06
Ho	0.29	0.28	0.61	0.18	0.68
Er	1.04	0.97	1.79	0.53	2.12
Tm	0.18	0.17	0.23	0.07	0.34
Yb	1.14	1.22	1.46	0.46	2.44
Lu	0.22	0.22	0.19	0.08	0.41
Hf	2.6	2.8	2.7	0.9	3.5
Ta	0.1	0.3	1.2	0.1	0.6
Th	4.0	7.4	63.6	5.0	14.9
U	2.4	1.9	32.7	0.7	6.2

4. Results

Samples for this study were collected from the M'Clintock West and M'Clintock East bodies of the Thores Suite. Five representative felsic to intermediate lithologies were chosen for further petrographic, geochemical and geochronological studies. The GPS coordinates and lithological type for each sample site are presented in Table 1. Outcrop photographs are shown in Fig. 2.

4.1. Petrography

All studied samples are coarse grained, holocrystalline igneous rocks (Fig. 3) that show small to intermediate degrees of alteration. Based on the petrographic observations they are classified as granite, quartz-monzonite, syenite and monzodiorite.

Sample KK17-10A is a granite that consists of anhedral plagioclase, microcline, quartz, biotite and white mica (Fig. 3A). Minor secondary zeolite, carbonate and epidote occur as well. Accessory phases are titanite, zircon and apatite. Plagioclase is altered and partly replaced by fine grained sericite. A sample of quartz monzonite, KK12-12G, consists mainly of alkali feldspar, sodic to calcic plagioclase, quartz, biotite and white mica (Fig. 3B). Accessory phases are represented by apatite and zircon. Biotite is rarely replaced by secondary chlorite. Late carbonate is locally present. Sample KK17-14C is classified as syenite and is the most altered sample examined. It consists mainly of alkali feldspar (sanidine) and plagioclase (Fig. 3C). Biotite, white mica, amphibole, epidote and secondary carbonate are also observed. Accessory phases include titanite, apatite and zircon. Plagioclase is extensively replaced by sericite. Biotite is commonly affected by chloritization. Sample KK17-15B is a monzodiorite. The major rock forming minerals are coarse grained plagioclase, green amphibole and alkali feldspar with lesser epidote, white mica, biotite, tourmaline and apatite (Figs. 3D,E). Plagioclase is commonly altered and locally replaced by opaque minerals (Fig. 3E). Finally, granite sample KK17-16A comprises similar minerals to KK17-10A. However, this sample has been affected by stronger deformation than the other samples, which is expressed by grain size reduction (especially quartz). The subhedral plagioclase is affected by sericitization, whereas biotite is locally replaced by chlorite.

4.2. Geochemistry

Geochemical data from five samples that are not significantly altered is plotted on several commonly used major and trace element diagrams used for classification and establishing the geotectonic setting (Fig. 4). The results of this study are plotted together with the only other available data from this region published by Trettin (1998) and Estrada et al. (2018a).

Based on the TAS diagram (Middlemost, 1994, Fig. 4A), the samples are classified as granite (KK17-10A, KK17-16A), syenite (KK17-14C), quartz monzonite (KK17-12G) and monzodiorite (KK17-15B), which is in agreement with the petrographic observations. The diagram of Schandl and Gorton (2002) indicates that the studied samples plot within the oceanic arc environment (Fig. 4B). All analyses plot within the volcanic arc granitoid field on the Pearce et al. (1984) diagram

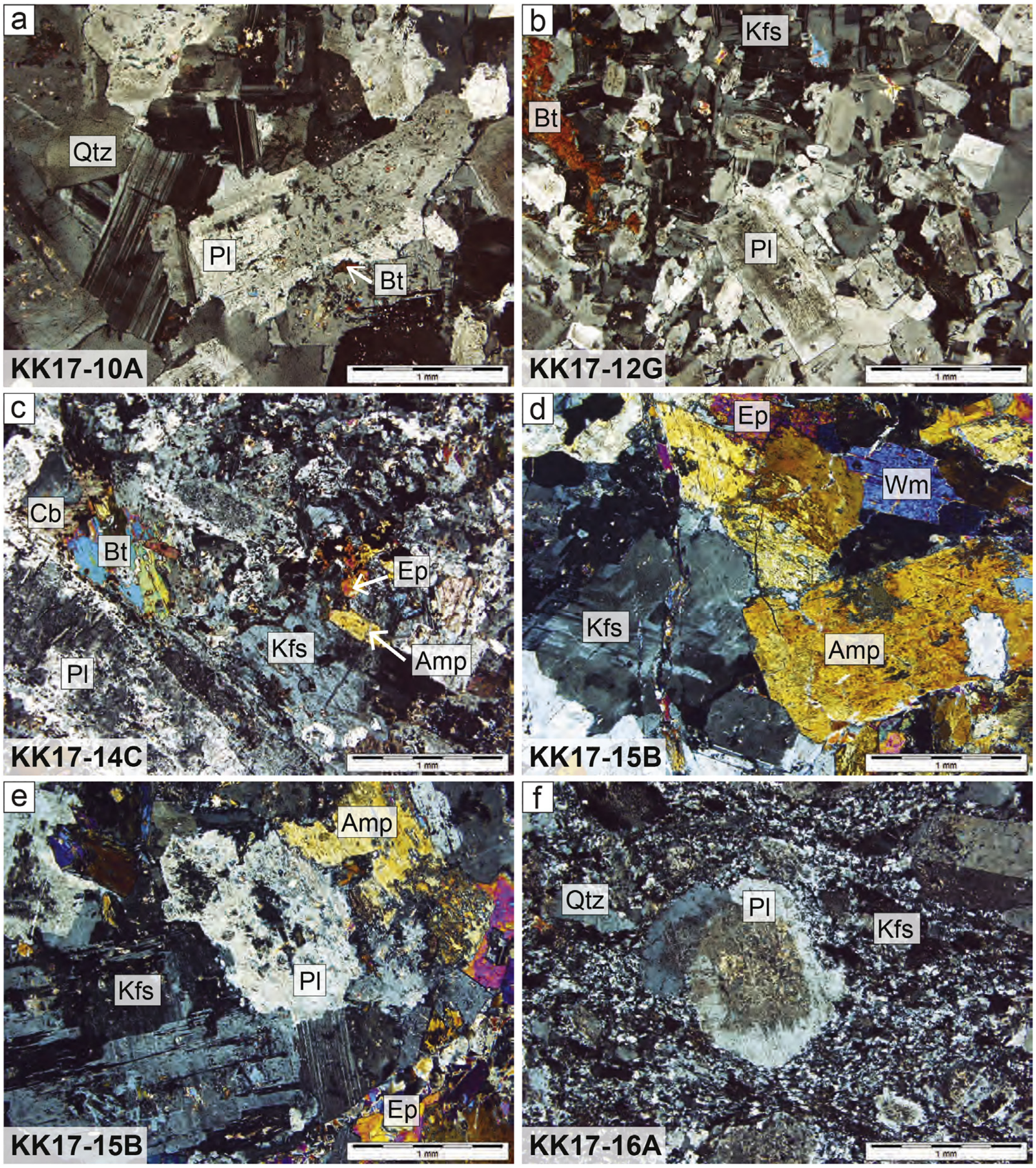

Fig. 3. Representative photomicrographs of the studied samples: (a) anhedral plagioclase from granite sample KK17-10A, (b) quartz monzonite sample KK17-12G comprising mainly plagioclase and alkali feldspar, (c) altered syenite sample KK17-14C - note mafic minerals: amphibole, biotite and epidote, (d) monzodiorite sample KK17-15B consisting mainly of felspar, plagioclase and amphibole, (e) plagioclase partly replaced by fine grain opaque minerals, the sample KK17-15B, (f) quartz, plagioclase and feldspar rich granite sample KK17-16A, plagioclase is commonly affected by sericitization. Abbreviations of mineral: Pl – plagioclase, Kfs – K-feldspar, Qtz – quartz, Bt – biotite, Wm- white mica, Ep - epidote, Amp – amphibole and Cb – carbonate.

(Fig. 4C). The results are consistent with evolution of the Thores Suite within a convergent tectonic environment.

The Thores Suite felsic to intermediate rocks show rather similar trend on the REE diagram (Boynton, 1984; Fig. 4D). They display an enrichment of light rare earth elements relative to heavy rare earth elements. The Eu anomaly is either absent to slightly negative (samples KK17-12G, KK17-16A) or positive (sample KK17-15B). All samples also show a similar trend on a multi-element diagram normalized to primitive mantle (McDonough and Sun, 1995; Fig. 4E). Notably the Ba, Rb, U and Th, LREE as well as Sr show distinct enrichment, whereas Nb–Ta and HREE show characteristic depletion. This trend is typical for an island arc environment. Similar trends and values have been reported for Andean type continental arc (e.g., Thorpe et al., 1984).

4.3. Geochronology

All five samples of intermediate to felsic lithologies contain zircon. Concentrations of Th in all dated zircons range between 15 and 1230 ppm, whereas U shows a spread from 62 to 4225 ppm (Supplementary Appendix A). The samples KK17-14C and KK17-15B yielded

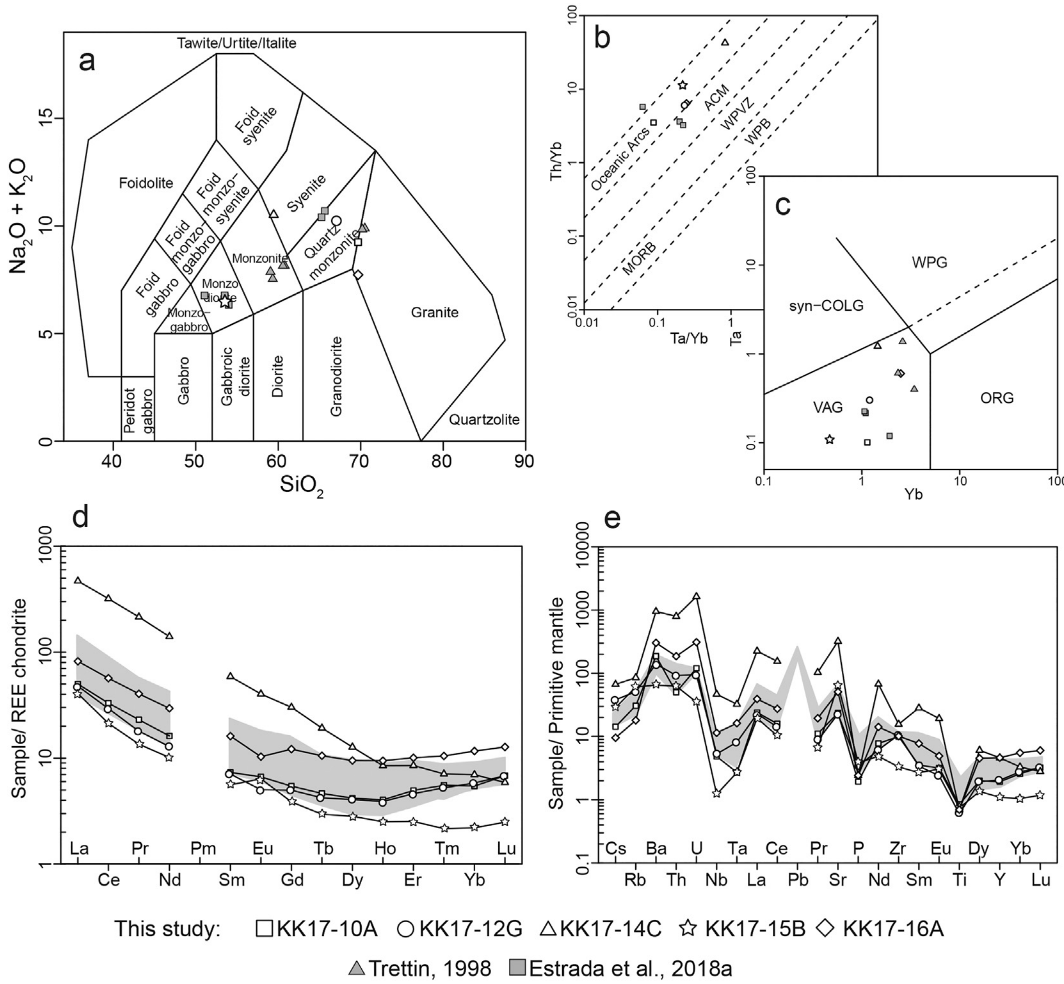

Fig. 4. Geochemistry of the studied samples. Following diagrams are shown: (a) TAS diagram (Middlemost, 1994), (b) Schandl and Gorton (2002) discrimination diagram (ACM – active continental margin, WPVZ – within plate volcanic zone, WPB – within plate basalts, MORB – mid-ocean ridge basalts), (c) Pearce et al. (1984) discrimination diagrams (*syn*-COLG – syncollisional granitoids, WPG – intraplate granitoids, ORG – mid-oceanic ridge granitoids, VAG – volcanic island arc granitoids), (d) Chondrite normalized REE plot (Boynton, 1984), (e) Primitive mantle normalized multi-element plot (McDonough and Sun 1995). The studied samples are marked as open symbols, whereas the grey symbols are the data from the literature: rectangles (Trettin, 1998) and triangles (Estrada, Tessensohn, and Sonntag, 2018b). The diagrams were prepared using GCDkit software (Janoušek et al., 2006).

subhedral, CL-dark zircon grains. Zircon in KK17-15B reveals weak oscillatory and sector zoning (Fig. 5). Zircon in KK17-14C has a mottled appearance and does not show any obvious zoning. Some grains from this sample display narrow CL-bright rims (Fig. 5). Zircon from the samples KK17-10A, KK17-12G and KK17-16A are euhedral, occasionally subround, oscillatory zoned with very clear, CL-bright cores and darker rims. All samples are characterized by bimodal size distribution of zircon grains with larger crystals not exceeding 300 μm in maximum dimension and smaller ones not exceeding 50 μm in diameter.

There is a significant spread in the U–Pb ages and degree of discordance within the analyzed samples that is interpreted to reflect the combined effects of Pb loss, inheritance and/or mix of inherited and magmatic components. The ^{206}Pb/^{238}U age of the magmatic zircons ranges between 480 ± 4 Ma and 469 ± 4 Ma (Fig. 6 and Appendix A). The older zircons are interpreted as inherited grains. They are recognized in the samples KK17-10A, KK17-12G and KK17-16A (see also Fig. 5 for CL images). The ^{206}Pb/^{238}U age for the younger xenocrystic grains range from 961 ± 10 Ma to 519 ± 6 Ma, the older inherited zircons yield ^{207}Pb/^{206}Pb ages between 2686 ± 9 Ma and 1045 ± 17 Ma (Fig. 7, Appendix A). The xenocrystic core dates cluster around 580–519 Ma (five grains), 625 (one grain) 890–792 Ma (thirteen grains), 1045–942 Ma (four grains), 1360 Ma and 1620 (each population one grain), 1865–1835 (two grains) as well as 2686–2455 Ma (eight grains). The distribution of inherited ages and probability plot for all 35 analyses are presented on Fig. 7.

Zircon from monzodiorite sample KK17-15B have a relatively simple age distribution and no inherited grains. The oldest 13 of 20 ^{207}Pb-corrected ^{206}Pb/^{238}U dates define a weighted mean age of 470 ± 3 Ma (MSWD = 1.5). The remaining dates ranging down to 430 Ma are interpreted to reflect Pb loss. Analyses from the sample of syenite, KK17-14C show a more significant spread of ^{207}Pb-corrected U–Pb ages from 488 to 262 Ma with no obvious inheritance. Most of the analyses are interpreted to record Pb loss. The oldest 6 analyses define a weighted mean ^{206}Pb/^{238}U age of 478 ± 6 Ma (MSWD = 1.0). All three samples KK17-10A, KK17-12G and KK17-16A show a large spread in U–Pb ages that coupled with the CL images is interpreted to reflect the combined effects of inheritance and Pb-loss (Fig. 5). Analyses from the granite sample KK17-10A vary from 2616 Ma to 325 Ma. Core analyses from inferred xenocrystic zircon show a U–Pb age spread from 2616 Ma to 528 Ma. Two older rim analyses (10.1 & 23.2) are interpreted to record analytical mixtures of rim and core domains. The 6 youngest analyses of the rims are interpreted to record Pb-loss. The remaining 4 rim analyses define a ^{207}Pb-corrected ^{206}Pb/^{238}U weighted mean age of 469 ± 4 Ma ($n = 4$ of 20, MSWD = 0.9). The quartz monzonite sample KK17-12G has a significant component of inherited cores as well. The core ages vary from 2686 Ma to 541 Ma although many of the analyses are discordant. Eleven

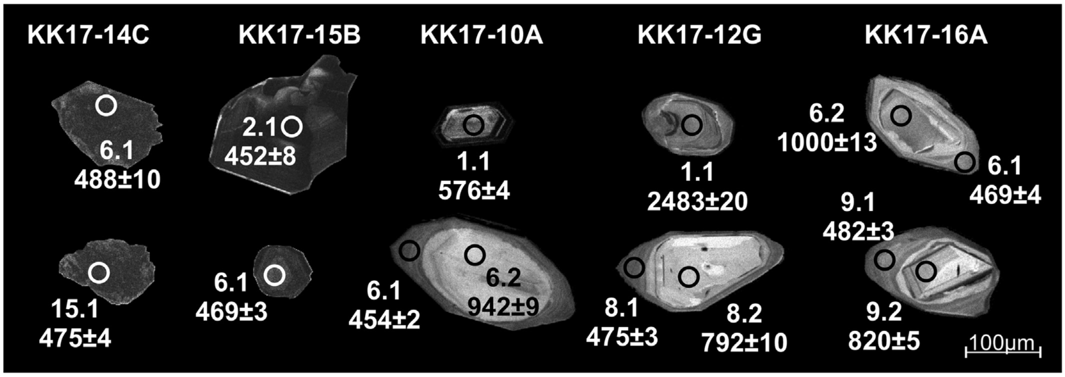

Fig. 5. Representative cathodoluminescence (CL) images of the analyzed zircon grains with spot locations marked by ellipses. U—Pb data are presented in Appendix A.

rim analyses give a ^{207}Pb-corrected ^{206}Pb/^{238}U weighted mean age of 480 ± 4 Ma (MSWD = 1.4, n = 11 of 35). The youngest two analyses are interpreted to record Pb-loss. Granite sample KK17-16A yielded the inherited cores ages ranging from 2457 Ma to 519 Ma. The oldest zircons are strongly discordant (>20%). Five younger analyses are inferred to record Pb-loss. The remaining zircon rims define a ^{207}Pb-corrected ^{206}Pb/^{238}U weighted mean age of 478 ± 4 Ma (MSWD = 1.7, n = 13 of 33).

5. Discussion

5.1. Age, petrogenesis and ancestry of the Thores Suite

Traditionally the Thores Suite was interpreted as a remnant of ophiolitic and plutonic complexes that originated above an intraoceanic subduction system formed in northern Iapetus (e.g. Trettin, 1998). Estrada et al., 2018b proposed a more complex model involving a build-up of an Ordovician island arc on a former late Neoproterozoic island arc of Timanian origin and its Cambrian sedimentary cover. The latter model is based largely on the age and character of various lithologies of Neoproterozoic and Cambrian meta-volcanosedimentary and sedimentary units of the Succession III in the Pearya Terrane. A critical assumption of the model is an intrusive relationship between the Thores Suite and the Neoproterozoic-Cambrian units of the Succession III even though (1) the contact is now most probably tectonic, and (2) there is no evidence for recycling of the Succession III (meta)sedimentary units in igneous rocks of the Thores Suite. The U–Pb data presented herein addresses the second concern since zircon from two granitic samples and a sample of quartz monzonite provide ages of inheritance ranging from c. 2680 Ma to c. 520 Ma. The age of the youngest inherited grain of 519 ± 6 Ma is older than the maximum deposition age of volcanoclastic sedimentary rocks of the Succession III, whereas the cluster around 580–570 Ma matches well 573 +6/−2 Ma weighted average of pyroclastic component in the same sequence (Estrada et al., 2018a). Thus the xenocryst data confirms that felsic to intermediate rocks of the Thores Suite may have indeed at least partially recycled the Cambrian to Neoproterozoic units of the Succession III. However, xenocryst ages older than c. 710 Ma (i.e. the oldest date yielded by the Succession III) require a more extensive evaluation of potential sources and allow additional examination into the origin of the composite arc fragment represented by Succession III and the Thores Suite.

The spread xenocryst ages clearly shows that at least some Thores Suite magmas intruded through heterogeneous Precambrian basement. The Neoarchean to earliest Neoproterozoic age signature is typically found in the circum-Arctic region (e.g. Olierook et al., 2020) and may be diagnostic for its provenance (e.g. Hadlari et al., 2014; Kirkland et al., 2009; Malone et al., 2014). For example, a gap in the obtained zircon age record, between 1620 Ma and 1360 Ma (but the dated population is limited), matches North American Magmatic Gap (1610–1490 Ma, Van Schmus et al., 1993), which suggests a Laurentian origin for the sampled basement. On the other hand, a cluster of c. 1040–940 Ma may equally be associated with both Laurentia and Baltica, either with a proposed Arctic arm of the Grenville-Sveconorwegian Orogen (Lorenz et al., 2012) or more likely the Valhalla Orogen, a convergent margin arc system developed on the external margin of Rodinia (Cawood et al., 2010). Igneous rocks of c. 974–964 Ma in Succession I of the Pearya Terrane are interpreted to record involvement of the Pearya Terrane in the Valhalla orogen (Malone et al., 2017). The presence of this age group in the Thores Suite xenocryst population suggests a primary tie between Succession III and other units of the Pearya Terrane with which it collided during the M'Clintock orogeny.

Even more interesting are latest Tonian to Cryogenian ages clustering between 890 Ma and 790 Ma and the Ediacaran population spanning 580–570 Ma. The younger cluster is typical for the Timanide Orogen of Baltica (e.g. Kuznetsov et al., 2007; Pease et al., 2004) as well as numerous peri-Gondwanan and peri-Laurentian terranes associated with the opening and closure of the Iapetus Ocean and evolution of the Appalachian orogen (van Staal et al., 2013, 2020 and references therein). Although direct ties between the northern Appalachian orogen and crustal fragments in the North Atlantic have been proposed (e.g., Pettersson et al., 2010), we view evolution of the Pearya Terrane in the more northern reaches of the Iapetan realm more likely and therefore focus on North Atlantic correlations. The possible north-western extension of the Timanides toward Svalbard and northern Greenland, potentially affecting the (future) northern Laurentian margin, was also proposed and documented (e.g. Estrada et al., 2018b; Kuznetsov et al., 2007; Majka et al., 2008, 2014,; Mazur et al., 2009; Rosa et al., 2016). Importantly, Malone and McClelland (2020) provide unequivocal evidence for the occurrence of c. 540 Ma intermediate, volcanic arc magmatism in the Pearya Terrane, which is based on U–Pb zircon dating coupled with trace-element and Hf isotopic analyses of the dated zircons. Thus, it is indeed likely that the spatial extent of the Timanide tectonism was much larger than hitherto recognized and could have spanned toward Laurentia sensu stricto or affected foundered blocks of continental crust possessing crustal signatures typical for Laurentia. It is also apparent that the Thores Suite igneous rocks intruded into and interacted with a basement that either included sedimentary units with similar detrital zircon signatures to the age pattern obtained from the inherited zircon cores in this study or consisted of a more structurally complex terrane comprising Neoarchean to latest Neoproterozoic or even Cambrian crystalline and sedimentary rocks. Interestingly, it supports a hypothesis of Hadlari et al. (2014) that the island arc in question might have been built upon the continental crust of Pearya, with the critical distinction that the Thores Suite records arc magmatism in the upper plate of a convergent margin setting distal to the northern Laurentian margin.

The geochemical character of the igneous rocks in the Thores Suite confirms their island arc affinity. The available geochronological constraints suggest this arc developed in the Early and Middle Ordovician, between c. 480 Ma and c. 469 Ma. The age of xenocrysts observed

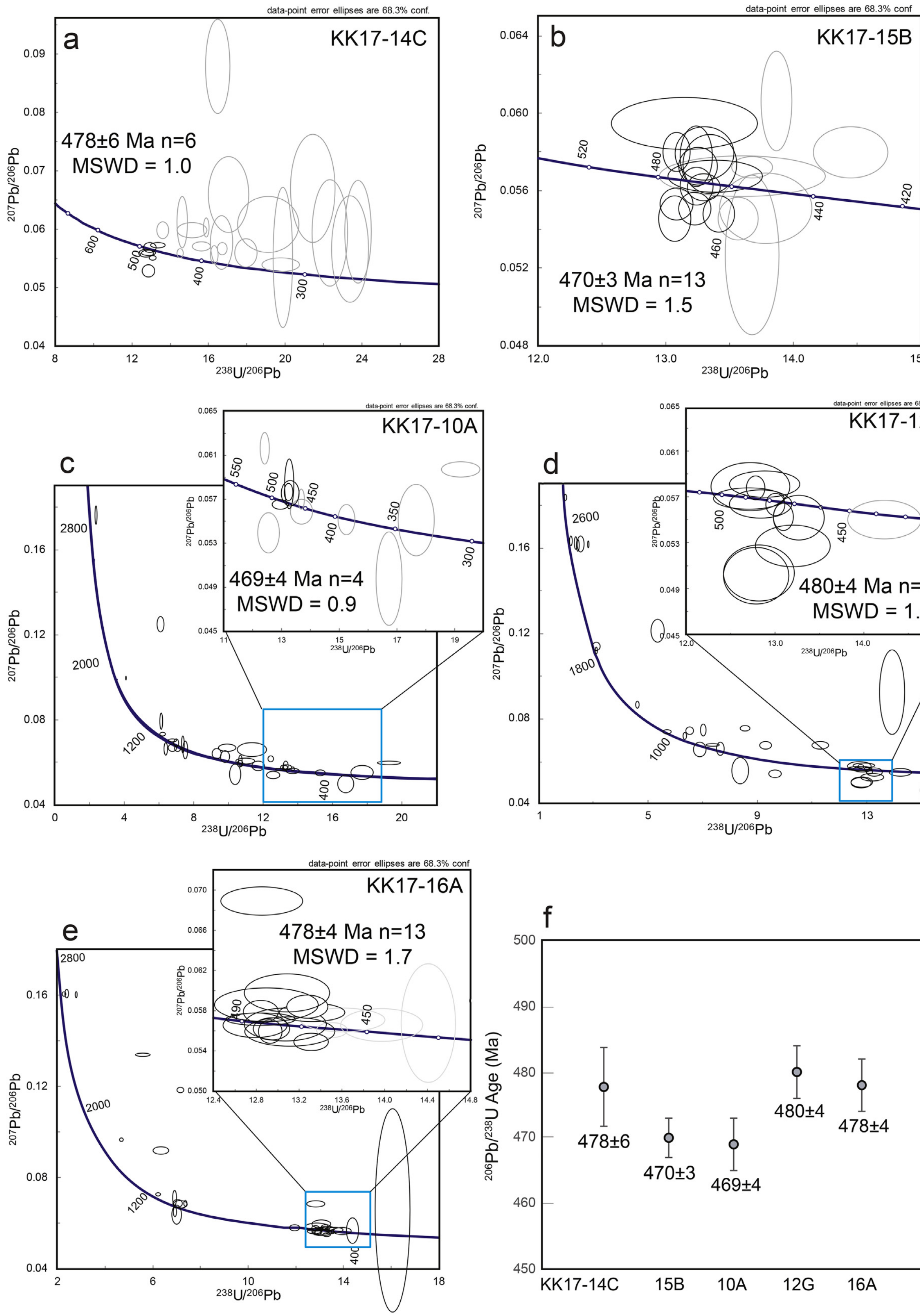

Fig. 6. Terra-Wasserburg plots. Data used for age calculations are marked by black ellipses. Grey ellipses indicate analyses not included in the age calculations due to the Pb loss, inheritance or mixed age, see text for more details. The plotted analyses are 1σ error ellipses uncorrected for common Pb.

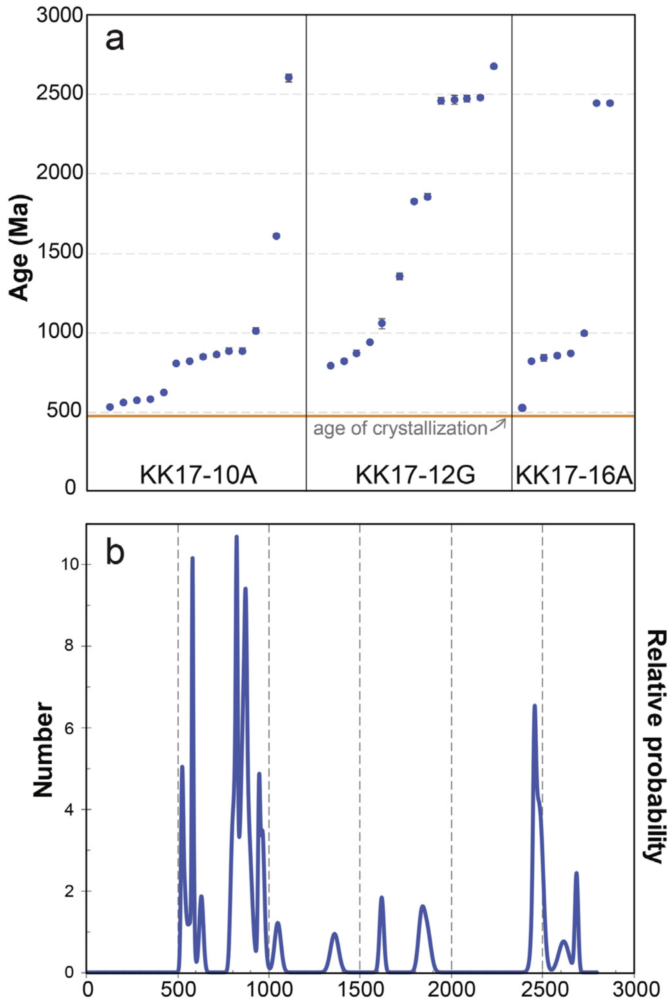

Fig. 7. (a) Diagram showing the distribution of xenocrystic zircon grains, crystallization age inferred for the studied samples is marked by orange line, (b) probability plot for all inherited zircons from samples KK17-10A, KK17-12G and KK17-16A. $^{207}Pb/^{206}Pb$ ages are shown for grains older than 1000 Ma and $^{206}Pb/^{238}U$ ages for younger zircons. The analyses plotted on both diagrams are 90–110% concordant for ages >1000 Ma and 80–120% concordant for ages <1000 Ma.

suggests that the arc formed on Laurentian crust or a fragment of Laurentian crust affected by late Neoproterozoic (Timanian?) tectonism. Development of an Early to Middle Ordovician arc along the Laurentian margin sensu stricto in the northern Iapetus realm has not been hitherto recognized, but has been proposed in models attempting to account for the origin of arc fragments from the Arctic region that are now included within the Cordilleran orogen (e.g., Strauss et al., 2017). In addition Dalslåen et al. (2020) suggested formation of an intraoceanic island arc proximal to the Laurentia margin by c. 487–480 Ma that is currently preserved within the Upper Allochthon of the central Norwegian Caledonides. A system of volcanic island arcs of a corresponding age that was particularly well developed along the Baltoscandian margin of Baltica also currently occurs within the Upper Allochthon of the Scandinavian Caledonides (e.g. Pickering and Smith, 1995; Roberts et al., 2010; Stephens and Gee, 1989). However, these arcs have an intra-oceanic origin and do not show any obvious evidence for a continental crustal component, which at first glance precludes any connection between the Thores Suite and the Upper Allochthon of the Scandinavian Caledonides. Therefore, an alternative tectonic mechanism allowing for a formation of an island arc built atop continental crust is necessary.

The earliest stages of opening of an infant ocean involve hyperextension and subsequent breakup of a continent. Rarely is newly formed ocean devoid of any slivers of continental crust imbedded within oceanic lithosphere (e.g., Jan Mayen microcontinent in Northern Atlantic; Gudlaugsson et al., 1988). Hyperextension of the Baltoscandian margin of Baltica was documented in detail (e.g. Andersen et al., 2012; Jakob et al., 2019) and proposed for segments of the Laurentian margin (van Staal et al., 2020), thus providing a viable mechanism for generation of continental fragments during rifting of Rodinia. A similar style of rifting is likely for the northern Laurentian margin as well (e.g., Strauss et al., 2019). Subduction initiation in northern Iapetus resulted in arc construction across both oceanic and rifted continental substrates leading to development of a composite intra-oceanic island arc system that includes continental crustal components.

The timing of rift and arc development in the northern Iapetus remain poorly constrained. The Thores Suite zircons yield inheritance ages as young as 580–570 Ma and c. 520 Ma which postdate traditional timing (630–600 Ma) for opening of the Iapetus Ocean (Johansson, 2009; Murphy et al., 2004; Torsvik et al., 1996). On the other hand, the Central Iapetus Magmatic Province (CIMP) was active until c. 550 Ma (Ernst and Bell, 2010). The Volyn Large Igneous province of southern Baltica operated between c. 580 Ma and c. 545 Ma (Compston et al., 1995; Paszkowski et al., 2019; Shumlyanskyy et al., 2016). Gumsley et al. (2020) reported occurrence of an alkali gabbro in the Caledonian basement of western Svalbard dated to c. 560 Ma and ascribed it to CIMP. The Seiland Igneous Province of the northernmost Scandinavian Caledonides yielded ages in the range of 574–526 Ma (Roberts et al., 2010). It is likely that this voluminous and predominantly mafic magmatism contributed to further dismembering of the Laurentian and Baltican continental crusts, which could have caused opening of marginal basins along continental margins similar to that envisioned for the Taconic seaway (e.g., Zagorevski and van Staal, 2011). In such a scenario, slivers of continental crust may have rifted away from either continental margin as late as the early Cambrian and shortly afterwards become basement for an intra-oceanic island arc.

In summary, it is apparent that the Thores Suite represents a remnant of intra-oceanic island arc presumably formed on a fragment of continental crust rifted from the Laurentian margin in the Ediacaran to the early Cambrian. This continental sliver must have been either affected by the Timanian metamorphic and/or magmatic event or covered by sedimentary units formed in the latest Neoproterozoic to earliest Cambrian (Fig. 8). The meta-volcanosedimentary units of Succession III of the Pearya Terrane may represent a partial remnant of the continental basement on which the Early to Middle Ordovician island arc formed. Intra-oceanic subduction beneath this continental sliver resulted in formation of the Thores volcanic arc in the Early Ordovician (Fig. 8). Possible candidates for the lower plate representatives (or their equivalents) are blueschists, low temperature eclogites and associated blueschist facies metasedimentary rocks of the Vestgötabreen Complex from Svalbard (Hirajima et al., 1988; Kośmińska et al., 2014) that yield Early to Middle Ordovician ages for HP metamorphism (Barnes et al., 2020; Bernard-Griffiths et al., 1993; Kośmińska et al., 2019; Peucat et al., 1989). Interestingly, HP zircon in these blueschists and eclogites reveals inheritance broadly similar to that described from the Thores Suite felsic rocks (Kośmińska et al., 2019). Subducted continental material that is age equivalent to the arc basement indicates subduction erosion such that the Vestgötabreen Complex is representative of the Thores Suite arc basement (Fig. 8). Other HP rocks known from the northernmost Iapetus realm are eclogites of the Richarddalen Complex in northern Svalbard. They are thought to have undergone HP metamorphism in the Middle Ordovician based on U–Pb dating of titanite (Gromet and Gee, 1998), although the currently available geochronological database is poor. The Richarddalen eclogites are embedded in a host dominated by Tonian to Cryogenian orthogneiss (Gromet and Gee, 1998; Peucat et al., 1989). A Tonian igneous suite, referred to as the Berzeliuseggene unit, records Torellian metamorphism, a Cryogenian tectonometamorphic event linked to Timanian tectonism, (see e.g. Majka and Kośmińska, 2017) as well as early Caledonian HP metamorphism that is was also described in southern Svalbard (Majka et al., 2014, 2015).

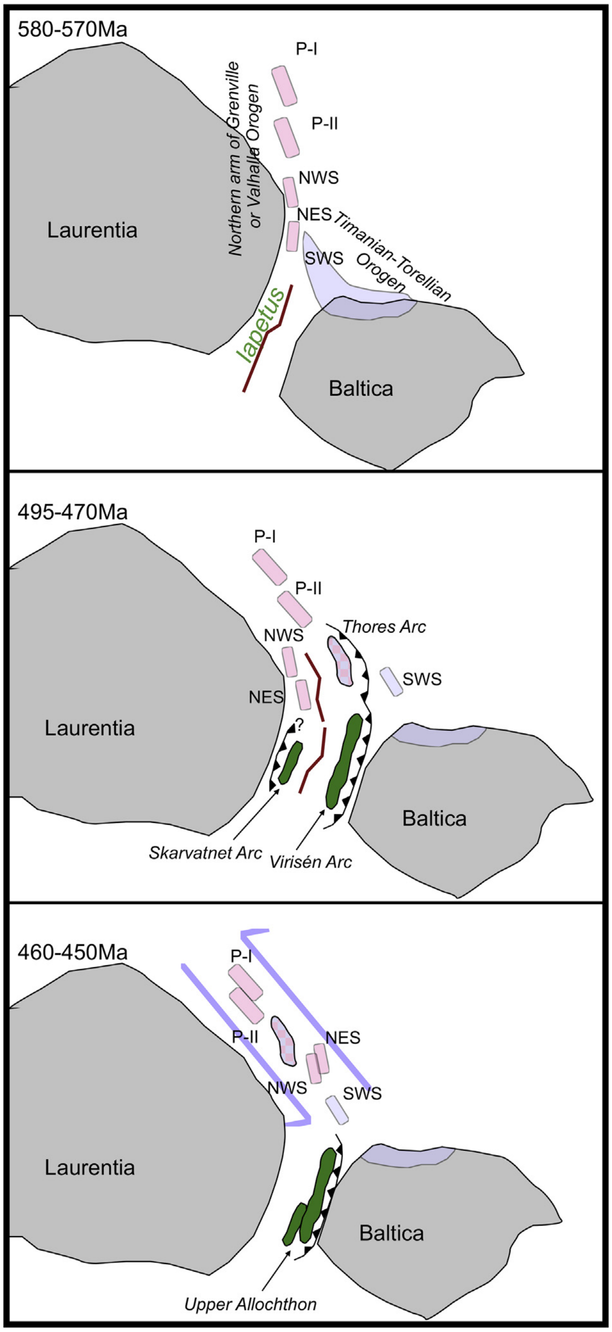

Fig. 8. A simplified cartoon showing hypothetical tectonic scenario for the development of the Thores island arc. Abbreviations used: NES – Northeastern Basement Province of Svalbard, NWS – Northwestern Basement Province of Svalbard, P-I – Pearya Succession I, P-II – Pearya Succession II, P-III – Pearya Succession III, SWS – Southwestern Basement Province of Svalbard.

Collectively, the Richarddalen Complex and Berzeliuseggene unit are interpreted to characterize the missing crustal puzzle piece that served as basement to the Thores Suite island arc (Fig. 8). However, more geochronologic and other isotope studies are required to target these units to unequivocally support this hypothesis.

5.2. The Thores Suite - the northernmost witness of the Caledonian contraction

Notwithstanding, the discussion presented above leads to an emerging question whether the M'Clintock orogenic event should be still treated as an independent entity or rather as one of multiple phases of Caledonian orogeny and in broader sense the Caledonian Wilson cycle. Elvevold et al. (2014) emphasized possible connection between the eclogites of the Richarddalen Complex and HP rocks of the Tromsø Nappe in the northernmost Norwegian Caledonides. Similarly, Barnes et al. (2020) showed striking similarities between coeval low temperature HP rocks of the Vestgötabreen Complex and from the Tsäkkok Lens of the Middle Allochthon of the Swedish Caledonides. Thus, it is justified to speculate that all these units could have formed in the same complex system of (multiple) intra-Iapetian island arcs. The arrival of the Baltoscandian continental margin into this complex subduction system in the south (i.e. in the northern Swedish and Norwegian segments of the Caledonides using current coordinates) would inhibit its further development in the north (Arctic-Barents segment of the Caledonides) and eventually cause its termination. The Baltoscandian margin subduction beneath an island arc in the northern and central Scandinavian Caledonides was already active at c. 495–470 Ma (e.g. Barnes et al., 2019; Bukała et al., 2020; Petrík et al., 2019), reaching its fully developed stage at c. 460–450 Ma (e.g. Brueckner and van Roermund, 2004; Fassmer et al., 2017). At the same time, the subduction system in the Arctic-Barents segment of the orogen would change its mode into transpression in much similar way to e.g. the Guatemala Suture currently separating the North American and Caribbean plates (e.g. Brueckner et al., 2009). Indeed, potential field interpretation presented by Barrère et al. (2009, 2011) shows a change in direction of the Caledonian suture in the Barents Sea region and it is interpreted to be an effect of left-lateral faulting (Barrère et al., 2011). Activation of this large, sinistral strike-slip system along the northeastern edge of Baltica was responsible for escape and juxtaposition of various crustal domains with differing histories including the mosaic of terranes currently exposed in Pearya and Svalbard (e.g. Bazarnik et al., 2019; Beranek et al., 2015; Colpron and Nelson, 2009; Malone et al., 2014; Mazur et al., 2009). This process could have started in the Ordovician (McClelland et al., 2012), continued at least until the late Silurian – Early Devonian (e.g. Faehnrich et al., 2020), and probably even beyond reaching the Late Devonian. In this model, juxtaposition of Successions I and II with Succession III of the Pearya Terrane would not reflect arc collision attributed to M'Clintock Orogenesis. Formation of the Thores Suite would reflect the early stages of the sensu stricto Caledonian orogenic contraction. This scenario links several tectonic phenomena commonly treated independently by various authors in the past and provides a plausible explanation for the currently observed basement architecture of this portion of the High Arctic. Nevertheless, additional geochronological and petrological investigations of all of the geological units discussed herein are needed to build a comprehensive tectonic model for evolution of Iapetus in this region.

6. Conclusions

The new ion microprobe U–Pb zircon dating results of various felsic to intermediate lithologies from the Thores Suite of the Succession III of the Pearya Terrane of northern Ellesmere Island support the following major conclusions:

(1) The dated samples of granites, quartz-monzonite, syenite and monzodiorite yielded igneous zircon ages ranging from 480 ± 4 Ma to 469 ± 4 Ma. These results extend the timing of igneous activity within the Thores Suite beyond the previous range of c. 488–481 Ma. Geochemical characteristics of the dated samples confirm volcanic island arc origin of the Thores Suite.
(2) Zircon from two granite samples and a sample of quartz-monzonite reveal inheritance interpreted to be characteristic of Laurentia with a c. 580–570 Ma component typical of the Timanide Orogen of northeast Baltica. Based on the occurrence of inherited zircon cores and their ages, it is suggested that the Thores Suite was formed in an island arc built on a sliver of continental crust within northern Iapetus.
(3) The age of the Thores Suite rocks matches ages of similar rocks

occurring within the Upper Allochthon of the Scandinavian Caledonides as well as of high pressure rocks from the Svalbard and northern Scandinavian Caledonides. Hence, the Thores island arc formed part of well-developed Early to Middle Ordovician Caledonian subduction system and should not be treated independently of it.

(4) Possible northern(most) location of the Thores island arc allowed its incorporation into large-scale sinistral strike slip-system responsible for escape and juxtaposition of terranes with mixed affinities. This system was already active during the early stages of the Baltica subduction beneath island arcs and fully developed during the main Caledonian continental collision between Baltica and Laurentia farther south. However, entirely Laurentian ancestry might be also considered as plausible.

Declaration of Competing Interest

We declare no conflict of interest.

Acknowledgements

This paper is dedicated to the memory of Prof. Jacek Rajchel, who sadly passed away last year. Some of us (KK, JB & JM) would never have been able to start working in the High Arctic without his pioneering, geological mapping of Wedel Jarlsberg Land, Spitsbergen. The research was supported by the National Science Centre (Poland) project no. 2015/17B/ST10/03114 to J. Majka, the internal grant of the Polish Geological Institute - NRI no. 62.9012.2014.00.0 to J. Bazarnik and National Science Foundation (USA) grant EAR1650022 to J. Gilotti and W. McClelland. The fieldwork was carried out during the Circum Arctic Structural Events CASE 19 Expedition organized by Federal Institute for Geosciences and Natural Resources (BGR Hannover, Germany) in 2017 led by Dr. Kartsen Piepjohn with a logistical support from the Polar Continental Shelf Program (PCSP). The authors would like to thank the helicopter pilot Rob Ferlisi for his assistance during sample collection, great sense of humor and unforgettable flights. Victoria Pease and an anonymous reviewer are acknowledged for their thoughtful reviews.

Appendix A. Supplementary data

Supplementary data to this article can be found online at https://doi.org/10.1016/j.lithos.2021.105999.

References

Andersen, T.B., Corfu, F., Labrousse, L., Osmundsen, P.T., 2012. Evidence for hyper - extension in the Pre-Caledonian continental margin of Baltica. Journal of the Geol. Soc. London. 14, 601–612. https://doi.org/10.1144/0016-76492012-011.Evidence.

Barnes, C., Majka, J., Schneider, D., Walczak, K., Bukała, M., Kośmińska, K., Tokarski, T., Karlsson, A., 2019. High-spatial resolution dating of monazite and zircon reveals the timing of subduction–exhumation of the Vaimok Lens in the Seve Nappe Complex (Scandinavian Caledonides). Contrib. Mineral. Petrol. 174, 0. https://doi.org/10.1007/s00410-018-1539-1.

Barnes, C.J., Walczak, K., Janots, E., Schneider, D., Majka, J., 2020. Timing of paleozoic exhumation and deformation of the high-pressure vestgötabreen complex at the Motalafjella Nunatak, Svalbard. Minerals 10, 1–23. https://doi.org/10.3390/min10020125.

Barrère, C., Ebbing, J., Gernigon, L., 2009. Offshore prolongation of Caledonian structures and basement characterisation in the western Barents Sea from geophysical modelling. Tectonophysics 470, 71–88. https://doi.org/10.1016/j.tecto.2008.07.012.

Barrère, C, Ebbing, J, Gerningon, L, 2011. 3-D density and magnetic crustal characterization of the southwestern Barents Shelf: implications for the offshore prolongation of the Norwegian Caledonides. Geophysical Journal International 184 (3), 1147–1166. https://doi.org/10.1111/j.1365-246X.2010.04888.x.

Bazarnik, J., Majka, J., McClelland, W.C., Strauss, J.V., Kośmińska, K., Piepjohn, K., Elvevold, S., Czupyt, Z., Mikuš, T., 2019. U-Pb zircon dating of metaigneous rocks from the Nordbreen Nappe of Svalbard's Ny-Friesland suggests their affinity to Northeast Greenland. Terra Nova 31, 518–526. https://doi.org/10.1111/ter.12422.

Beranek, L.P., Pease, V., Hadlari, T., Dewing, K., 2015. Silurian flysch successions of ellesmere island, arctic canada, and their significance to northern caledonian palaeogeography and tectonics. J. Geol. Soc. Lond. 172, 201–212. https://doi.org/10.1144/jgs2014-027.

Bernard-Griffiths, J., Peucat, J.J., Ohta, Y., 1993. Age and nature of protoliths in the Caledonian blueschist-eclogite complex of western Spitsbergen: a combined approach using UPb, SmNd and REE whole-rock systems. Lithos 30, 81–90. https://doi.org/10.1016/0024-4937(93)90007-Y.

Black, L.P., Kamo, S.L., Allen, C.M., Aleinikoff, J.N., Davis, D.W., Korsch, R.J., Foudoulis, C., 2003. TEMORA 1: A new zircon standard for Phanerozoic U-Pb geochronology. Chem. Geol. 200, 155–170. https://doi.org/10.1016/S0009-2541(03)00165-7.

Black, L.P., Kamo, S.L., Allen, C.M., Davis, D.W., Aleinikoff, J.N., Valley, J.W., Mundil, R., Campbell, I.H., Korsch, R.J., Williams, I.S., Foudoulis, C., 2004. Improved 206Pb/238U microprobe geochronology by the monitoring of a trace-element-related matrix effect; SHRIMP, ID-TIMS, ELA-ICP-MS and oxygen isotope documentation for a series of zircon standards. Chem. Geol. 205, 115–140. https://doi.org/10.1016/j.chemgeo.2004.01.003.

Boynton, William V., 1984. Cosmochemistry of the Rare Earth Elements: Meteorite Studies. In: Henderson, P. (Ed.), Developments in Geochemistry, Elsevier, Volume 2, pp. 63–114. https://doi.org/10.1016/B978-0-444-42148-7.50008-3.

Brueckner, H.K., Avé Lallemant, H.G., Sisson, V.B., Harlow, G.E., Hemming, S.R., Martens, U., Tsujimori, T., Sorensen, S.S., 2009. Metamorphic reworking of a high pressure-low temperature mélange along the Motagua fault. Guatemala: A record of Neocomian and Maastrichtian transpressional tectonics. Earth Planet. Sci. Lett. 284, 228–235. https://doi.org/10.1016/j.epsl.2009.04.032.

Brueckner, H.K., van Roermund, H.L.M., 2004. Dunk tectonics: A multiple subduction/eduction model for the evolution of the Scandinavian Caledonides. Tectonics 23, 1–20. https://doi.org/10.1029/2003TC001502.

Bukała, M., Majka, J., Walczak, K., Włodek, A., Schmitt, M., Zagórska, A., 2020. U-pb zircon dating of migmatitic paragneisses and garnet amphibolite from the high pressure seve nappe complex in Kittalfjäll. Swedish caledonides. Minerals 10. https://doi.org/10.3390/min10040295.

Cawood, P.A., Strachan, R., Cutts, K., Kinny, P.D., Hand, M., Pisarevsky, S., 2010. Neoproterozoic orogeny along the margin of Rodinia: Valhalla orogen, North Atlantic. Geology 38, 99–102. https://doi.org/10.1130/G30450.1.

Colpron, M., Nelson, J.L., 2009. A Palaeozoic Northwest Passage: Incursion of Caledonian, Baltican and Siberan terranes into eastern Panthalassa, and the early evolution of the North American Cordillera. Geol. Soc. Spec. Publ. 318, 273–307. https://doi.org/10.1144/SP318.10.

Compston, W., Sambridge, M.S., Reinfrank, R.F., Moczydłowska, M., Vidal, G., Claesson, C.S., 1995. Late precambrian volcanics of Poland.pdf. J. Geol. Soc. 152, 599–611. https://doi.org/10.1144/gsjgs.152.4.0599.

Dalslåen, B.H., Gasser, D., Grenne, T., Augland, L.E., Andresen, A.A., 2020. Early-Middle Ordovician sedimentation and bimodal volcanism at the margin of Iapetus: the Trollhøtta–Kinna Basin of the central Norwegian Caledonides. Geol. Soc. London, Spec. Publ. 503. doi.10.1144/SP503-2020-37

Elvevold, S., Ravna, E.J.K., Nasipuri, P., Labrousse, L., 2014. Calculated phase equilibria for phengite-bearing eclogites from NW Spitsbergen, svalbard caledonides. Geol. Soc. Spec. Publ. 390, 385–401. https://doi.org/10.1144/SP390.4.

Ernst, R.E., Bell, K., 2010. Large igneous provinces (LIPs) and carbonatites. Mineral. Petrol. 98, 55–76. https://doi.org/10.1007/s00710-009-0074-1.

Estrada, S., Mende, K., Gerdes, A., Gärtner, A., Hofmann, M., Spiegel, C., Damaske, D., Koglin, N., 2018a. Proterozoic to Cretaceous evolution of the western and central Pearya Terrane (Canadian High Arctic). J. Geodyn. 120, 45–76. https://doi.org/10.1016/j.jog.2018.05.010.

Estrada, S., Tessensohn, F., Sonntag, B.L., 2018b. A Timanian island-arc fragment in North Greenland: The Midtkap igneous suite. J. Geodyn. 118, 140–153. https://doi.org/10.1016/j.jog.2018.01.015.

Faehnrich, K., Majka, J., Schneider, D., Mazur, S., Manecki, M., Ziemniak, G., Wala, V.T., Strauss, J.V., 2020. Geochronological constraints on Caledonian strike–slip displacement in Svalbard, with implications for the evolution of the Arctic. Terra Nova 32, 290–299. https://doi.org/10.1111/ter.12461.

Fassmer, K., Klonowska, I., Walczak, K., Andersson, B., Froitzheim, N., Majka, J., Fonseca, R.O.C., Münker, C., Janák, M., Whitehouse, M., 2017. Middle Ordovician subduction of continental crust in the Scandinavian Caledonides: an example from Tjeliken, Seve Nappe Complex. Sweden. Contrib. to Mineral. Petrol. 172. https://doi.org/10.1007/s00410-017-1420-7.

Gee, D.G., Janák, M., Majka, J., Robinson, P., van Roermund, H., 2013. Subduction along and within the baltoscandian margin during closing of the Iapetus ocean and baltica-laurentia collision. Lithosphere 5, 169–178. https://doi.org/10.1130/L220.1.

Gee, D.G., Teben'kov, A.M., 2005. Svalbard: A fragment of the Laurentian margin. Geol. Soc. Mem. 30, 191–206. https://doi.org/10.1144/GSL.MEM.2004.030.01.16.

Gromet, L.P., Gee, D.G., 1998. An evaluation of the age of high-grade metamorphism in the Caledonides of BiskayerhalvØya, NW Svalbard. Gff 120, 199–208. https://doi.org/10.1080/11035899801202199.

Gudlaugsson, S.T., Gunnarsson, K., Sand, M., Skogseid, J., 1988. Tectonic and volcanic events at the Jan Mayen Ridge microcontinent. Geol. Soc. Spec. Publ. 39, 85–93. https://doi.org/10.1144/GSL.SP.1988.039.01.09.

Gumsley, A., Manby, G., Domańska-Siuda, J., Nejbert, K., Michalski, K., 2020. Caught between two continents: First identification of the Ediacaran Central Iapetus Magmatic Province in Western Svalbard with palaeogeographic implications during final Rodinia breakup. Precambrian Res., 341 https://doi.org/10.1016/j.precamres.2020.105622.

Hadlari, T., Davis, W.J., Dewing, K., 2014. A pericratonic model for the Pearya terrane as an extension of the Franklinian margin of Laurentia, Canadian Arctic. Bull. Geol. Soc. Am. 126, 182–200. https://doi.org/10.1130/B30843.1.

Hirajima, T., Banno, S., Hiroi, Y., Ohta, Y., 1988. Phase petrology of eclogites and related rocks from the Motalafjella high-pressure metamorphic complex in Spitsbergen

(Arctic Ocean) and its significance. Lithos 22, 75–97. https://doi.org/10.1016/0024-4937(88)90018-7.
Jakob, J., Andersen, T.B., Kjøll, H.J., 2019. A review and reinterpretation of the architecture of the South and South-Central Scandinavian Caledonides—A magma-poor to magma-rich transition and the significance of the reactivation of rift inherited structures. Earth-Science Rev. 192, 513–528. https://doi.org/10.1016/j.earscirev.2019.01.004.
Janoušek, V., Farrow, C.M., Erban, V., 2006. Interpretation of Whole-rock Geochemical Data in Igneous Geochemistry: Introducing Geochemical Data Toolkit (GCDkit). J. Petrol. 47, 1255–1259.
Johansson, Å., 2009. Baltica, Amazonia and the SAMBA connection-1000 million years of neighbourhood during the Proterozoic? Precambrian Res. 175, 221–234. https://doi.org/10.1016/j.precamres.2009.09.011.
Kirkland, C.L., Pease, V., Whitehouse, M.J., Ineson, J.R., 2009. Provenance record from Mesoproterozoic-Cambrian sediments of Peary Land, North Greenland: Implications for the ice-covered Greenland Shield and Laurentian palaeogeography. Precambrian Res. 170, 43–60. https://doi.org/10.1016/j.precamres.2008.11.006.
Kośmińska, K., Majka, J., Mazur, S., Krumbholz, M., Klonowska, I., Manecki, M., Czerny, J., Dwornik, M., 2014. Blueschist facies metamorphism in Nordenskiöld Land of west-central Svalbard. Terra Nova 26, 377–386. https://doi.org/10.1111/ter.12110.
Kośmińska, K., McClelland, W.C., Majka, J., Fassmer, K., Coble, M.A., 2019. U-Pb and Lu-Hf geochronology of blueschist and eclogite from the Vestgötabreen Complex, Svalbard. IEC 2019: 13th International Eclogite Conference: Petrozavodsk, Russia, June. 24–27, p. 2019.
Kuznetsov, N.B., Soboleva, A.A., Udoratina, O.V., Hertseva, M.V., Andreichev, V.L., 2007. Pre-Ordovician tectonic evolution and volcano-plutonic associations of the Timanides and northern Pre-Uralides, northeast part of the East European Craton. Gondwana Res. 12, 305–323. https://doi.org/10.1016/j.gr.2006.10.021.
Labrousse, L., Elvevold, S., Lepvrier, C., Agard, P., 2008. Structural analysis of high-pressure metamorphic rocks of Svalbard: Reconstructing the early stages of the Caledonian orogeny. Tectonics 27, 1–22. https://doi.org/10.1029/2007TC002249.
Lorenz, H., Gee, D.G., Larionov, A.N., Majka, J., 2012. The Grenville-Sveconorwegian orogen in the high Arctic. Geol. Mag. 149, 875–891. https://doi.org/10.1017/S0016756811001130.
Ludwig, R.K., 2000. SQUID 1.00. Berkeley Geochronol. Cent. Spec. Publ. 2, 17.
Ludwig, R.K., 2003. User's Manual for a Geochronological Toolkit for Microsoft Excel (Isoplot/Ex Version 3.0). Berkeley Geochronol. Cent. Spec. Publ. 1–70.
Majka, J., Be'Eri-Shlevin, Y., Gee, D.G., Czerny, J., Frei, D., Ladenberger, A., 2014. Torellian (c. 640 Ma) metamorphic overprint of Tonian (c. 950 Ma) basement in the Caledonides of southwestern Svalbard. Geol. Mag. 151, 732–748. https://doi.org/10.1017/S0016756813000794.
Majka, J., Kośmińska, K., 2017. Magmatic and metamorphic events recorded within the Southwestern Basement Province of Svalbard. Arktos 3, 1–7. https://doi.org/10.1007/s41063-017-0034-7.
Majka, J., Kośmińska, K., Mazur, S., Czerny, J., Piepjohn, K., Dwornik, M., Manecki, M., 2015. Two garnet growth events in polymetamorphic rocks in southwest spitsbergen, norway: Insight in the history of neoproterozoic and early paleozoic metamorphism in the high arctic. Can. J. Earth Sci. 52, 1045–1061. https://doi.org/10.1139/cjes-2015-0142.
Majka, J., Mazur, S., Manecki, M., Czerny, J., Holm, D.K., 2008. Late Neoproterozoic amphibolite-facies metamorphism of a pre-Caledonian basement block in southwest Wedel Jarlsberg Land, Spitsbergen: New evidence from U-Th-Pb dating of monazite. Geol. Mag. 145, 822–830. https://doi.org/10.1017/S001675680800530X.
Malone, S.J., McClelland, W.C., 2020. Zircon geochronology and geochemistry of the Ward Hunt pluton, Pearya terrane, Canadian High Arctic: Insights into its age, origin, and circum-Arctic Timanide connections. Arktos 6, 93–105. https://doi.org/10.1007/s41063-020-00078-9.
Malone, S.J., McClelland, W.C., von Gosen, W., Piepjohn, K., 2014. Proterozoic evolution of the north Atlantic–Arctic Caledonides: Insights from detrital zircon analysis of metasedimentary rocks from the Pearya terrane, Canadian high arctic. J. Geol. 122, 623–648. https://doi.org/10.1086/677902.
Malone, S.J., McClelland, W.C., von Gosen, W., Piepjohn, K., 2017. The earliest Neoproterozoic magmatic record of the Pearya terrane, Canadian high Arctic: Implications for Caledonian terrane reconstructions. Precambrian Res. 292, 323–349. https://doi.org/10.1016/j.precamres.2017.01.006.
Mazur, S., Czerny, J., Majka, J., Maneck, M., Holm, D., Smyrak, A., Wypych, A., 2009. A strike-slip terrane boundary in Wedel Jarlsberg Land, Svalbard, and its bearing on correlations of SW Spitsbergen with the Pearya terrane and Timanide belt. J. Geol. Soc. Lond. 166, 529–544. https://doi.org/10.1144/0016-76492008-106.
McClelland, W.C., Malone, S.J., von Gosen, W., Piepjohn, K., Läufer, A., 2012. Die zeitliche einordnung der sinistralen Verschiebung des Pearya-Terranes entlang des randes der kanadischen Arktis. Zeitschrift der Dtsch. Gesellschaft fur Geowissenschaften 163, 251–259. https://doi.org/10.1127/1860-1804/2012/0163-0251.
McDonough, W.F., Sun S.-s., 1995. The composition of the Earth. Chem. Geol. 120 (3-4), 223–253.
Middlemost, A.E.K., 1994. Naming materials in the magma/igneous rock system. Earth-Sci. Rev. 37, 215–224.
Murphy, J.B., Fernández-Suárez, J., Keppie, J.D., Jeffries, T.E., 2004. Contiguous rather than discrete Paleozoic histories for the Avalon and Meguma terranes based on detrital zircon data. Geology 32, 585–588. https://doi.org/10.1130/G20351.1.
Nawrocki, J., Gozhik, P., Łanczont, M., Pańczyk, M., Komar, M., Bogucki, A., Williams, I.S., Czupyt, Z., 2018. Palaeowind directions and sources of detrital material archived in the Roxolany loess section (southern Ukraine). Palaeogeogr. Palaeoclimatol. Palaeoecol. 496, 121–135. https://doi.org/10.1016/j.palaeo.2018.01.028.
Olierook, H.K.H., Jourdan, F., Whittaker, J.M., Merle, R.E., Jiang, Q., Pourteau, A., Doucet, L.S., 2020. Timing and causes of the mid-Cretaceous global plate reorganization event. Earth Planet. Sci. Lett. 534, 116071. https://doi.org/10.1016/j.epsl.2020.116071.
Paszkowski, M., Budzyń, B., Mazur, S., Sláma, J., Shumlyanskyy, L., Środoń, J., Dhuime, B., Kędzior, A., Liivamägi, S., Pisarzowska, A., 2019. Detrital zircon U-Pb and Hf constraints on provenance and timing of deposition of the Mesoproterozoic to Cambrian sedimentary cover of the East European Craton. Belarus. Precambrian Res. 331. https://doi.org/10.1016/j.precamres.2019.105352.
Pearce, J.A., Harris, N.B.W., Tindle, A.G., 1984. Trace element discrimination diagrams for the tectonic interpretation of granitic rocks. J. Petrol. 25, 956–983. https://doi.org/10.1093/petrology/25.4.956.
Pease, V., Dovzhikova, E., Beliakova, L., Gee, D.G., 2004. Late Neoproterozoic granitoid magmatism in the basement to the Pechora Basin, NW Russia: geochemical constrains indicate westward sudduction beneath NE Baltica. In: Gee, D.G., Pease, V. (Eds.), The Neoproterozoic Timanide Orogen of Eastern Baltica. Geol. Soc. Lond. Mem. 30, pp. 75–85.
Petrík, I., Janák, M., Klonowska, I., Majka, J., Froitzheim, N., Yoshida, K., Sasinková, V., Konečný, P., Vaculovič, T., 2019. Monazite Behaviour during Metamorphic Evolution of a Diamond-bearing Gneiss: A Case Study from the Seve Nappe Complex, Scandinavian Caledonides. J. Petrol. 60, 1773–1796. https://doi.org/10.1093/petrology/egz051.
Pettersson, C.H., Pease, V., Frei, D., 2010. Detrital zircon U/Pb ages of Silurian-Devonian sediments from NW Svalbard: a fragment of Avalonia and Laurentia?: Journal of the Geological Society. London. 167, 1019–1032.
Peucat, J.J., Ohta, Y., Gee, D.G., Bernard-Griffiths, J., 1989. U-Pb, Sr and Nd evidence for grenvillian and latest proterozoic tectonothermal activity in the spitsbergen caledonides, arctic ocean. Lithos 22, 275–285. https://doi.org/10.1016/0024-4937(89)90030-3.
Pickering, K.T., Smith, A.G., 1995. Arcs and backarc basins in the Early Paleozoic lapetus Ocean. Island Arc 4, 1–67. https://doi.org/10.1111/j.1440-1738.1995.tb00132.x.
Roberts, R.J., Corfu, F., Torsvik, T., Hetherington, C.J., Ashwal, L.D., 2010. Age of alkaline rocks in the Seiland Igneous Province, Northern Norway. J. Geol. Soc. London 167, 71–81.
Rosa, D., Majka, J., Thrane, K., Guarnieri, P., 2016. Evidence for Timanian-age basement rocks in North Greenland as documented through U-Pb zircon dating of igneous xenoliths from the Midtkap volcanic centers. Precambrian Res. 275, 394–405. https://doi.org/10.1016/j.precamres.2016.01.005.
Schandl, E.S., Gorton, M.P., 2002. Application of high field strength elements to discriminate tectonic settings in VMS environments. Econ. Geol. 97, 629–642. https://doi.org/10.2113/gsecongeo.97.3.629.
Shumlyanskyy, L., Nosova, A., Billström, K., Söderlund, U., Andréasson, P.G., Kuzmenkova, O., 2016. The U–Pb zircon and baddeleyite ages of the Neoproterozoic Volyn Large Igneous Province: implication for the age of the magmatism and the nature of a crustal contaminant. Gff 138, 17–30. https://doi.org/10.1080/11035897.2015.1123289.
Stephens, M.B., Gee, D.G., 1989. Terranes and polyphase accretionary history in the Scandinavian Caledonides, in R.D. Dallmeyer ed., Terranes in the Circum-Atlantic Paleozoic Orogens: Geological Society of America 17–30. doi.10.1130/SPE230-p17
Strauss, J.V., Hoiland, C.W., Ward, W., Johnson, B.G., Nelson, L., McClelland, W.C., 2017. Orogen transplant: Taconic–Caledonian magmatism in the Brooks Range of Alaska: Geological Society of America Bulletin, 129, 649–676. https://doi.org/10.1130/B31593.1.
Strauss, J.V., Macdonald, F.A., McClelland, W.C., 2019. Pre-Mississippian stratigraphy and provenance of the North Slope subterrane of Arctic Alaska I: Platformal carbonate rocks of the northeastern Brooks Range and their significance in circum-Arctic evolution. In: Piepjohn, K., Strauss, J.V., Reinhardt, L., McClelland, W.C. (Eds.), Circum-Arctic Structural Events: Tectonic Evolution of the Arctic Margins and Trans-Arctic Links with Adjacent Orogens: Geological Society of America Special Paper. 541, pp. 493–524. https://doi.org/10.1130/2018.2541(22).
Thorpe, R.S., Francis, P.W., O'Callaghan, L., 1984. Relative roles of source composition, fractional crystalliza-tion and crustal contamination in the petrogenesis of An-dean volcanic rocks. Philos. Trans. R. Soc. Lond. A310, 675–692.
Torsvik, T.H., Smethurst, M.A., Meert, J.G., Van Der Voo, R., McKerrow, W.S., Brasier, M.D., Sturt, B.A., Walderhaug, H.J., 1996. Continental break-up and collision in the Neoproterozoic and Palaeozoic - A tale of Baltica and Laurentia. Earth-Science Rev. 40, 229–258. https://doi.org/10.1016/0012-8252(96)00008-6.
Trettin, H.P., 1991. The Geology of North America. vol. E. Geology of the Innuitian Orogen and Arctic Platform of Canada and Greenland, Geological Society of America, Boulder, CO, USA.
Trettin, H.P., 1998. Pre-Carboniferous geology of the northern part of the Arctic Islands: Northern Heiberg Fold Belt, Clements Markham Fold Belt, and Pearya; northern Axel Heiberg and Ellesmere islands.
Trettin, H.P., Loveridge, W.D., Sullivan, R.W., 1982. U/Pb ages on zircons from the M'Clintock West massif and the Markham Fiord pluton, northernmost Ellesmere Island. Curr. Res. Part C, Geol. Soc. Canada Pap 82 (1C), 161–166.
Trettin, H.P., Mayr, U., 1996. Geology, M'Clintock Inlet, District of Franklin, Northwest Territories. Geological Survey of Canada, Map 1882A, scale 1:250 000.
Van Schmus, W.R., Bickford, M.E., Anderson, J.L., Bender, E.E., Anderson, R.R., Bauer, P.W., Robertson, J.M., Bowring, S.A., Condie, K.C., Denison, R.E., Gilbert, M.C., Grambling, J.A., Mawer, C.K., Shearer, C.K., Hinje, W.J., Karlstrom, K.E., Kisvarsanyi, E.B., Lidiak, E.G., Reed Jr., J.C., Sims, P.K., Tweto, O., Silver, L.T., Treves, S.B., Williams, M.L., Wooden, J.L., 1993. In: Precambrian Conterminous, U.S., Reed Jr., J.C., Bickford, M.E., Houston, R.S., Link, P.K., Rankin, D.W., Sims, P.K., Van Schmus, W.R. (Eds.), Transcontinental Proterozoic provinces. vol. C-2. Geological Society of America, Geology of North America, pp. 171–334.

van Staal, C.R., Barr, S.M., Mccausland, P.J.A., Thompson, M.D., White, C.E., 2020. Tonian–Ediacaran tectonomagmatic evolution of West Avalonia and its Ediacaran–early Cambrian interactions with Ganderia: an example of complex terrane transfer due to arc–arc collision? In: Murphy, J.B., Strachan, R.A., Quesada, C. (Eds.), Pannotia to Pangaea: Neoproterozoic and Paleozoic Orogenic Cycles in the Circum-Atlantic Region. 503. Geological Society, London, Special Publications. https://doi.org/10.1144/SP503-2020-23

van Staal, C.R., Chew, D.M., Zagorevski, A., McNicoll, V., Hibbard, J., Skulski, T., Castonguay, S., Escayola, M.P., Sylvester, P.J., 2013. Evidence of Late Ediacaran Hyperextension of the Lau-rentian Iapetan Margin in the Birchy Complex, Baie Verte Peninsula, Northwest Newfoundland: Implica-tions for the Opening of Iapetus, Formation of Peri-Laurentian Microcontinents and Taconic – Grampian Orogenesis: Geoscience Canada. 40 pp. 94–117 10.12789.

Wiedenbeck, M., Alle, P., Corfu, F., Griffin, W.L., Meier, M., Oberli, F., von Quadt, A., Roddick, J.C., S, W., 1995. Three natural zircon standards for U-Th-Pn, Lu-Hf, trace element and REE analyses. Geostand. Newslett. 19, 1–23.

Wiedenbeck, M., Hanchar, J.M., Peck, W.H., Sylvester, P., Valley, J., Whitehouse, M., Kronz, A., Morishita, Y., N, L., 2004. Further Characterisation of the 91500 Zircon Crystal. Geostand. Geoanal. Res. 28, 9–39.

Williams, I.S., 1998. U-Th-Pb geochronology by ion microprobe. Appl. Microanal. Tech. to Underst. Miner. Process. 7, 1–35. https://doi.org/10.5382/rev.07.

Williams, I.S., Claesson, S., 1987. Isotopic evidence for the Precambrian provenance and Caledonian metamorphism of high grade paragneisses from the Seve Nappes. Scandinavian Caledonides - II. Ion microprobe zircon U-Th-Pb. Contrib. to Mineral. Petrol. 97, 205–217. https://doi.org/10.1007/BF00371240.

Zagorevski, A., van Staal, C.R., 2011. The record of Ordovician arc-arc and arc-continent collisions in the Canadian Appalachians during the closure of Iapetus –Chapter 12. In: Brown, D., Ryan, P.D. (Eds.), Arc-Continent Collision, Frontiers in Earth Sciences. Springer Verlag, Berlin Heidelberg, pp. 341–371. https://doi.org/10.1007/978-3-540-88558-0_12.